SIAM J. APPL. MATH.
Vol. 30, No. 1, January 1976

MATHEMATICAL MODEL OF THE COCHLEA. II: RESULTS AND CONCLUSIONS*

R. S. CHADWICK†, A. INSELBERG‡ AND K. JOHNSON¶

Abstract. A mathematical cochlear model with uniform geometrical and elastic properties is analyzed. The major emphasis is placed on relating the structure of the cochlea to its function. A Place principle is shown to exist when defined in terms of the position of the maxima of the wave envelopes of the basilar membrane. In contrast to previous thought, the viscosity of the inner ear fluid plays an important role in increasing tonal localization. The major effect of basilar membrane taper is to improve the low frequency response by shifting the low frequency envelope maxima toward the apical portion of the cochlea, which results in increased sensitivity to tonal differentiation. Explicit relations are given for low and high frequency auditory thresholds defined in terms of sensitivity. The low frequency threshold is affected only by the geometry of the basilar membrane, while all model parameters affect the high frequency threshold. For some values of the model parameters, "hearing defects" can be simulated.

Introduction. Previously [1], a mathematical model of the cochlea was formulated and the solution of the resulting equations of motion was obtained. Here the qualitative and quantitative results stemming from the solution function as well as their implications to physiological acoustics are discussed. Also included are some conclusions delimiting areas for further research.

1. Qualitative results.

1.1. Motion of the basilar membrane. The function, $\eta(x, t)$, describing the oscillations of the basilar membrane model [1, (28)], is conveniently represented by

$$\eta(x, t) = \eta_{ST}(x, t) + \eta_{TR}(x, t), \tag{1}$$

where the subscripts ST and TR denote the steady state and transient parts, respectively. In particular,

$$\eta_{ST}(x, t) = \sum_{n=1}^{\infty} (d_{1n} \sin \omega t + d_{2n} \cos \omega t) \sin \frac{n\pi x}{L} \tag{2}$$

and

$$\eta_{TR}(x, t) = -\sum_{n=1}^{\infty} e^{-\lambda_n t} \left(\frac{\lambda_n d_{2n} + \omega d_{1n}}{E_n} \sin E_n t + d_{2n} \cos E_n t \right) \sin \frac{n\pi x}{L}, \tag{3}$$

with the notation already given in [1].

The critically damped case occurs when $E_n = 0$, and it affects only the transient portion of $\eta(x, t)$, resulting in

$$\eta_{TR}(x, t) = -\sum_{n=1}^{\infty} e^{-\lambda_n t} [d_{2n} + (\omega d_{1n} + \lambda_n d_{2n})t] \sin \frac{n\pi x}{L} \tag{4}$$

when $E_n = 0$.

* Received by the editors July 24, 1973, and in final revised form September 30, 1974. This research was supported in part by IBM Corp. and in part by the Technion Research Foundation.

† Faculty of Mechanical Engineering, Technion-Israel Institute of Technology, Haifa, Israel.

‡ Department of Applied Mathematics, Technion-Israel Institute of Technology, Haifa, Israel. Now at IBM Scientific Center, Los Angeles, California 90067.

¶ IBM Scientific Center, Los Angeles, California 90067.

1.2. On resonance. It will be shown that, as in the human basilar membrane, the basilar membrane model has no real and positive resonant frequencies. This is in contrast to Huxley [2], who was led to believe that resonance can exist in the cochlea.

Resonance can only occur when the denominator

$$\Delta_n = (C_n - \omega^2 A_n)^2 + \omega^2 B_n^2 \tag{5}$$

of d_{in}, $i = 1, 2$, is equal to zero. To examine the zeros of (5), note that B_n contains $\omega^{1/2}$ through γ and r.

Write

$$\Delta_n = (C_n - \omega^2 A_n)^2 + \omega^3 b_n^2, \tag{6}$$

where now each one of the coefficients of powers of ω in (6) is independent of ω.

Consider

$$\omega^3 b_n^2 = -(C_n - \omega^2 A_n)^2$$

which implies that if ω is real, then $\omega \leqq 0$ since the right-hand side is $\leqq 0$ for all n. Clearly $\omega = 0$ cannot be a zero of Δ_n which provides the assertion stated at the beginning of this subsection. Negative frequencies are, of course, physically inadmissible.

1.3. Place principle and time envelopes of the oscillations. Originally, the Place principle in physiological acoustics held that every discriminable tone has its own distinctive position of activity in the basilar membrane. In precise language, this means that there exists a one-to-one correspondence between sound frequencies and positions on the basilar membrane [1, part (e) of the Introduction]. A generally accepted modern version of this principle is that there is no precise specificity of tonal action. Rather, every tone spreads its effects through the cochlea. The high tones have oscillation patterns for which the maximum activity occurs in the basal region, while the low tones have broader patterns with maxima close to the apical end. The region of most vigorous activity shifts towards the basal end as the frequency of the external signal increases. The present form of the Place principle plays a central role in auditory theory [3, pp. 400–402].

It is natural to study the Place principle by observing the oscillations for all times $t > 0$, which is equivalent to looking at the time envelopes of the oscillations, i.e., to specifically examine the position $x_{\max}$ of the maximum of the envelopes as a function of the input frequency ω [4, pp. 446–462].

Fortunately, a relatively simple formula for the time envelopes is obtained by observing that the time envelopes of the oscillations $\eta(x, t)$ are given by the time envelopes of the steady state part $\eta_{ST}(x, t)$. That is, the transient portion makes no contribution to the time envelopes. This is because $\eta_{TR}(x, t)$ reaches its maximum at $t = 0$ (see also § 2) progressively decaying as $t \to \infty$. The initial condition

$$\eta(x, 0) = 0$$

implies that

$$\eta_{ST}(x, 0) = -\eta_{TR}(x, 0),$$

which, together with the periodicity with respect to t of $\eta_{ST}(x, t)$, in turn implies that

$$\max_{t \geqq 0} |\eta(x, t)| = \max_{t \geqq 0} |\eta_{ST}(x, t)|$$

since

$$\max_{t \geqq 0} |\eta_{TR}(x, t)| = |\eta_{TR}(x, 0)|.$$

Returning to (2), and putting it in the form

$$\eta_{ST}(x, t) = a_1(x) \sin \omega t + a_2(x) \cos \omega t,$$

where

$$a_i(x) = \sum_{n=1}^{\infty} d_{in} \sin \frac{n\pi x}{L}, \qquad i = 1, 2, \tag{7}$$

yields

$$\eta_{ST}(x, t) = A(x) \sin (\omega t + \theta(x)), \tag{8}$$

where

$$\theta(x) = \sin^{-1} \frac{a_2(x)}{A(x)} = \cos^{-1} \frac{a_1(x)}{A(x)}$$

and

$$A(x) = [a_1^2(x) + a_2^2(x)]^{1/2}. \tag{9}$$

That is, $\eta_{ST}(x, t)$ consists of traveling waves having maximum amplitude $A(x)$. The expression $\eta_E(x)$ for the time envelopes of $\eta(x, t)$ is then simply

$$\eta_E(x) = \pm A(x).$$

The time envelopes of the oscillations are examined quantitatively and in detail in § 2.

In the remainder of this section, certain important asymptotic (with respect to ω) properties of $\eta_E(x)$ are shown. These properties pertain to the existence of high and low frequency thresholds and specifically relate to the behavior of the *position* $x_{\max}$ of the maximum of $\eta_E(x)$ as a function of ω. (See also the $x_{\max}$ vs. ω curves in § 2.)

Since the envelopes are symmetrical with respect to the x-axis, only the upper half $A(x) \geqq 0$ will be considered in the remainder of § 1.

1.4. The Place principle for high frequencies. As ω increases,

$$d_{1n} \to -\frac{D_n}{A_n} \frac{1}{\omega^2} \quad \text{and} \quad d_{2n} \to -\frac{b_n D_n}{A_n^2} \frac{1}{\omega^{5/2}},$$

where $B_n = \omega^{1/2} b_n$.

For all ω the positions x_E of the extrema of the envelopes are given by

$$\frac{dA(x_E)}{dx} = 0. \tag{10}$$

From (9),

$$A(x)A'(x) = a_1(x)a_1'(x) + a_2(x)a_2'(x); \tag{11}$$

therefore

$$a_1(x_E)a_1'(x_E) + a_2(x_E)a_2'(x_E) = 0. \tag{12}$$

The roots of (12), which also satisfy

$$A(x_E) = 0, \tag{13}$$

are excluded. In particular, the endpoints $x = 0$ and $x = L$ are two such cases. The endpoints, however, cannot satisfy (10), for if they did, this would imply that

$$\eta_x(0, t) = \eta_x(L, t) = 0, \qquad t \geqq 0,$$

which in turn implies that the basilar membrane is clamped at both ends. This, of course, is not the case in this model. Rather, the basilar membrane is supported by fixed hinges. Hence

$$A''(0) = A''(L) = 0.$$

The acceptable roots of (12) are those which correspond to waveforms (oscillations of the basilar membrane) having no fixed nodes in time.

For large ω, (12) approaches

$$A_1(x_E)A_1'(x_E) + \frac{1}{\omega}A_2(x_E)A_2'(x_E) = 0, \tag{14}$$

where $a_1(x) = (1/\omega^2)A_1(x)$ and $a_2(x) = (1/\omega^{5/2})A_2(x)$ with $A_i(x)$, $i = 1, 2$, being independent of ω.

Incidentally, (14) shows that

$$x_E = x_E(\omega),$$

which for the case when $A(x)$ has a relative maximum at x_E is the Place principle.

Differentiating now (14) with respect to ω yields

$$\frac{dx_E}{d\omega} = \frac{1}{\omega^2}\frac{A_2A_2'}{A_\infty}, \tag{15}$$

where

$$A_\infty = A_1A_1'' + (A_1')^2 + \frac{1}{\omega}(A_2A_2'' + (A_2')^2).$$

Note that for ω large, in view of (11),

$$AA'' + (A')^2 = A_\infty.$$

However, for x_E,

$$A'(x_E) = 0,$$

and

$$A''(x_E) = \frac{A_\infty(x_E)}{A(x_E)},$$

with $A(x_E) > 0$.

Now if x_E is the position of a relative maximum (write $x_{\max}$),

$$A''(x_{\max}) < 0,$$

which implies that

$$A_\infty(x_{\max}) < 0. \tag{16}$$

From (14) and (15),

$$\frac{dx_E}{d\omega} = -\frac{1}{\omega}\frac{A_1 A_1'}{A_\infty}. \tag{17}$$

The series $A_1(x)$ is easily summed. To wit, since

$$A_1(x) = B\sum_{n=1}^{\infty}\frac{n}{n^2+k^2}\sin\frac{n\pi x}{L}, \tag{18}$$

where

$$B = -\frac{2P_0\beta}{\alpha^2\pi}, \qquad k^2 = \frac{\beta L^2\rho_f}{\alpha^2\pi^2 h},$$

$$A_1(x) = B\sinh\left[\pi k\left(1-\frac{x}{L}\right)\right]. \tag{19}$$

Hence, for $0 \leqq x \leqq L$,

$$A_1(x)A_1'(x) < 0. \tag{20}$$

From (16), (17) and (20), then

$$\frac{dx_{\max}}{d\omega} = -\frac{1}{\omega}\frac{A_1(x_{\max})A_1'(x_{\max})}{A_\infty(x_{\max})} < 0 \qquad \text{for } \omega < \infty. \tag{21}$$

This leads to some fundamental conclusions, namely,

(i) $\dfrac{dx_{\max}}{d\omega} \to 0$ as $\omega \to \infty$,

(ii) $x_{\max} \downarrow \omega$ and, in fact, $x_{\max} \to 0$ as $\omega \to \infty$.

This is precisely the Place principle behavior for high frequencies as it has been observed experimentally.

Also, from (i) it is seen that *the sensitivity of the basilar membrane as a frequency analyzer diminishes as the frequency increases. Hence, past some frequency, frequency changes can no longer be detected. That is, there exists a high frequency threshold.*

The rate of change of $x_{\max}$ for large ω is given by (21). The right-hand side of (21) depends on the properties of the system (i.e., E, ρ, ρ_b, ν, h, d and L). Therefore (21) provides an explicit relationship between the high frequency threshold and sensitivity and the physical properties and geometry of the model.

1.5. Envelopes at low frequencies. As $\omega \to 0$, $A(x) \to |a_1(x)|$ with $d_{1n} = D_n/C_n$ since $d_{2n} \to 0$. The resulting sine series for the envelopes is

$$A(x) = c \sum_{n=1}^{\infty} \frac{L^5}{n^5\pi^5} \sin \frac{n\pi x}{L}, \tag{22}$$

where $c = -2P_0\beta/L$.

By means of a known summation formula [5] and some obvious manipulations,

$$A(u) = -\frac{c}{240}u(u-1)\left(u^3 - 4u^2 - \frac{8}{3}u + \frac{8}{3}\right), \tag{23}$$

where $u = x/L$, is obtained.

Equation (23) provides the shape of the envelopes as $\omega \to 0$. It is important to understand this as a limit since at $\omega = 0$ the system is actually not in motion. The function given by (23) resembles somewhat the sine function for half a period. (See low frequency envelope in Fig. 3.) This function has a single maximum (to four significant figures) at $u = 0.4807$.

Therefore

$$x_{MO} = \lim_{\omega \to 0} x_{\max}(\omega) = 0.4807L. \tag{24}$$

This confirms and improves a previous result [6], namely, that x_{MO} depends only on the length of the basilar membrane.

This result can also be obtained by appealing directly to the physics of the system. To wit, as $\omega \to 0$, the tangential shear stress $\tau \to 0$ since it is proportional to $\omega^{1/2}$. The dominant load on the basilar membrane is then the net pressure $p(x, t)$ which is given by [1, (30)]. It is not difficult to see that as $\omega \to 0$,

$$p(x, t) \to P_0\left(1 - \frac{x}{L}\right) \sin \omega t. \tag{25}$$

It turns out [7] that the deflection for such a load (within a frequency dependent factor) is also given by (23) with the position of the maximum deflection being independent of ω. In fact, the maximum deflection occurs precisely at x_{MO}. This confirms also the physical argument. Additionally, it provides a crucial clue. Since the load (25) at low frequencies is independent of the properties of the cochlea (i.e., fluid properties and dimensions), the resulting deflection can only depend on the elastic properties of the basilar membrane. This, of course, is still true for the *position* of maximum deflection. Hence, *at low frequencies, the Place principle is determined primarily by the stiffness (geometry) of the basilar membrane.* The high frequency behavior by contrast (see § 1.4 and § 2) is determined by the interaction of all properties of the system and particularly the fluid properties.

Consider again the load given by (25) (see Fig. 1). *The only way for x_{MO} to be close to the helicotrema ($x = L$), as the Place principle at low frequencies dictates, is by way of the basilar membrane having a substantially decreasing stiffness towards the helicotrema.* This is actually the case for the real basilar membrane. The taper in the basilar membrane then is needed for optimal low frequency behavior.

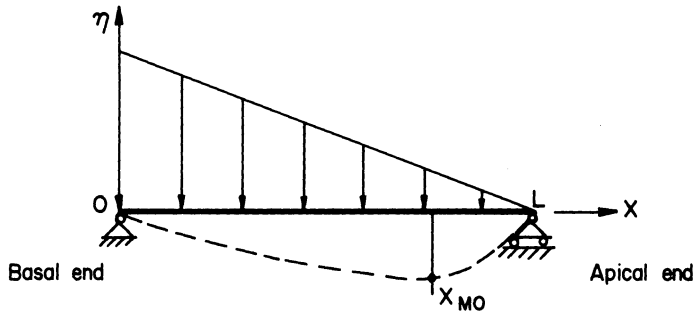

FIG. 1. *Load on basilar membrane at low frequencies*

A uniform basilar membrane provides excellent high frequency response (§ 2), but rather poor low frequency response.

These results together with an additional result on sensitivity at low frequencies (given in § 1.6) delimit the role of the stiffness gradient and geometry of the basilar membrane. In addition, they provide valuable insight about the tapered structure of the actual cochlea (see § 3).

1.6. Place principle at low frequencies. The analysis proceeds as in § 1.4. As $\omega \to 0$,

$$d_{1n} \to \frac{D_n}{C_n}\left(1 + \omega^2 \frac{A_n}{C_n}\right), \qquad d_{2n} \to -\omega^{3/2} \frac{b_n D_n}{C_n^2}. \tag{26}$$

The equation for the envelopes approaches

$$A^2(x) = (A_{10}(x) + \omega^2 A_{11}(x))^2 + \omega^3 A_2^2, \tag{27}$$

where

$$A_{10}(x) = \sum_{n=1}^{\infty} \frac{D_n}{C_n} \sin \frac{n\pi x}{L}, \qquad A_{11}(x) = \sum_{n=1}^{\infty} \frac{D_n A_n}{C_n^2} \sin \frac{n\pi x}{L} \tag{28}$$

and

$$A_2(x) = -\sum_{n=1}^{\infty} \frac{b_n D_n}{C_n^2} \sin \frac{n\pi x}{L}$$

are all independent of ω.

Recall also from § 1.5 that

$$\lim_{\omega \to 0} x_{\max}(\omega) = x_{MO} = 0.4807L.$$

From (27), where the prime indicates differentiation with respect to x,

$$AA' = A_{10}A'_{10} + \omega^2(A_{11}A'_{10} + A_{10}A'_{11}) + \omega^3 A_2 A'_2 + \omega^4 A_{11}A'_{11}. \tag{29}$$

This being a polynomial in ω (of degree four), there exists a neighborhood $N(0; r_1)$ of $\omega = 0$ where the sign of AA' is determined by the first two terms. Write

$$\text{sign}\,[AA'] = \text{sign}\,[A_{10}A'_{10} + \omega^2(A_{11}A'_{10} + A'_{11})] \tag{30}$$

$\forall\, \omega \in N(0; r_1)$.

From (30) for $A' = 0$,

$$A_{10}A'_{10} + \omega^2(A_{11}A'_{10} + A_{10}A'_{11}) = 0, \tag{31}$$

this being the condition for a local extremum of the envelope A for $(x = x_E)$, $\omega \in N(0; r_1)$, and $x_E \in N(x_{MO}; r_2)$.

From (29), differentiating with respect to x, we see there exists a neighborhood $N(0; r_3)$ of $\omega = 0$ (and a neighborhood $N(x_{MO}; r_4)$ such that

$$\operatorname{sign}(AA'' + (A')^2) = \operatorname{sign}[A_{10}A''_{10} + \omega^2(A_{10}A''_{11} + A_{11}A''_{10} + 2A'_{11}A'_{10}) + (A'_{10})^2] \tag{32}$$
$$\forall\, x \in N(x_{MO}; r_4), \quad \omega \in N(0; r_3).$$

Hence for $x_E \in N(x_{MO}; r'_2)$ and $\omega \in N(0; r'_1)$ where

$$r'_1 = \min(r_1, r_3), \qquad r'_2 = \min(r_2, r_4),$$

both (31) and (32) are valid. In fact, $A'(x_E) = 0$ and

$$A(x_{\max})A''(x_{\max}) < 0. \tag{33}$$

(Always $x_{\max}$ denotes the position of a local maximum of $A(x)$.)

Now differentiating (31) with respect to ω at $x_E = x_{\max}(\omega)$,

$$A(x_{\max})A''(x_{\max})\frac{dx_{\max}}{d\omega} = -2\omega(A_{11}A'_{10} + A_{10}A'_{11}), \tag{34}$$

where the coefficient of the right-hand side is evaluated at $x_{\max}(\omega)$,

From (34), an important conclusion can be made when it is realized that

$$A_{10}(x) = \lim_{\omega \to 0} A(x) \tag{35}$$

(this limiting envelope having already been discussed in § 1.5) and that $A_{11}(x)$ is also a polynomial in x.[1]

Since $x_{\max} \in [0, L]$, $\forall\, \omega \geqq 0$, $A_{11}A'_{10}$, $A_{10}A'_{11}$ are therefore bounded.

Hence, in view of (33) from (34), it is seen that

$$\lim_{\omega \to 0} \frac{dx_{\max}}{d\omega} = 0. \tag{36}$$

Furthermore, from (31) and (34),

$$A(x_{\max})A''(x_{\max})\frac{dx_{\max}}{d\omega} = \frac{2A_{10}(x_{\max})A'_{10}(x_{\max})}{\omega}; \tag{37}$$

this expression yields the sensitivity of the basilar membrane for small but not zero ω.

The function $A_{10}(x)$ (see (35)) is known from § 1.5. It has a single maximum at $x = x_{MO}$ and

$$A'_{10}(x) > 0 \quad \text{if } 0 \leqq x < x_{MO},$$
$$A'_{10}(x) < 0 \quad \text{if } x_{MO} < x \leqq L.$$

[1] In fact, $A_{11}(x)$ can be summed to give a polynomial of degree 10.

It is immediately seen that

$$\frac{dx_{\max}}{d\omega} < 0 \quad \text{if } x_{\max} < x_{MO}$$

$$\Rightarrow x_{\max} \downarrow \omega \Rightarrow x_{\max} \to x_{MO}^{-} \text{ as } \omega \to 0,$$

$$\frac{dx_{\max}}{d\omega} > 0 \quad \text{if } x_{\max} > x_{MO}$$

$$\Rightarrow x_{\max} \uparrow \omega \Rightarrow x_{\max} \to x_{MO}^{+} \quad \text{as } \omega \to 0.$$

Therefore, depending on the parameter values of the model, $x_{\max} \to x_{MO}$ either from the left or the right of x_{MO} monotonically as $\omega \to 0$. This is clearly indicated in Fig. 6.

From (35), just as in the case for high frequencies, it is seen that *there exists a low frequency threshold.*

The sensitivity of the basilar membrane model at low frequencies is given explicitly by (37). As it was seen in § 1.5, $A_{10}(x)$ depends primarily on the geometry of the basilar membrane. *The sensitivity, then, at low frequencies depends mostly on the geometry of the basilar membrane.* The high frequency sensitivity, by contrast (see § 1.3), depends on all the model properties.

The above conclusions confirm and improve substantially the results in [6]. There is corraborating evidence supporting these conclusions. A phenomenon called presbycusis occurs in which, with aging, a person's high frequency threshold diminishes. It is quite likely that with aging, E, the Young's modulus of the basilar membrane, changes and affects one's hearing. This change, according to our conclusions, would affect only the high frequency threshold. By contrast, in Meniere's disease, the basilar membrane is deformed due to an additional load on it. This, as has been shown above, should affect the low frequency threshold, which is precisely what has been observed clinically.

2. Quantitative results. The quantitative behavior of the model is shown in Figs. 2–7. In general, all the results presented were obtained only after a great deal of numerical experimentation with the parameters. Although it is possible to reduce the number of parameters by using nondimensional combinations, it was found that by specifying their values separately, it was easier to obtain more meaningful results. The model exhibits a wide variety of characteristics in different regions of the parameter space. This not only indicates that the model is versatile, but more important, that the real cochlea can function properly only over very narrow ranges of the parameter values.

The curves selected for presentation stress that a Place principle exists for a basilar membrane modeled as a beam with uniform geometrical and elastic properties. However, this uniformity results in an inefficient use of the beam as a frequency analyzer; i.e., envelope maxima occur only on the left half of the beam for those parameter settings which admit a Place principle. A Place principle is obtained with values of the geometrical parameters that can be identified with average values in a human cochlea. The values used in the computations are

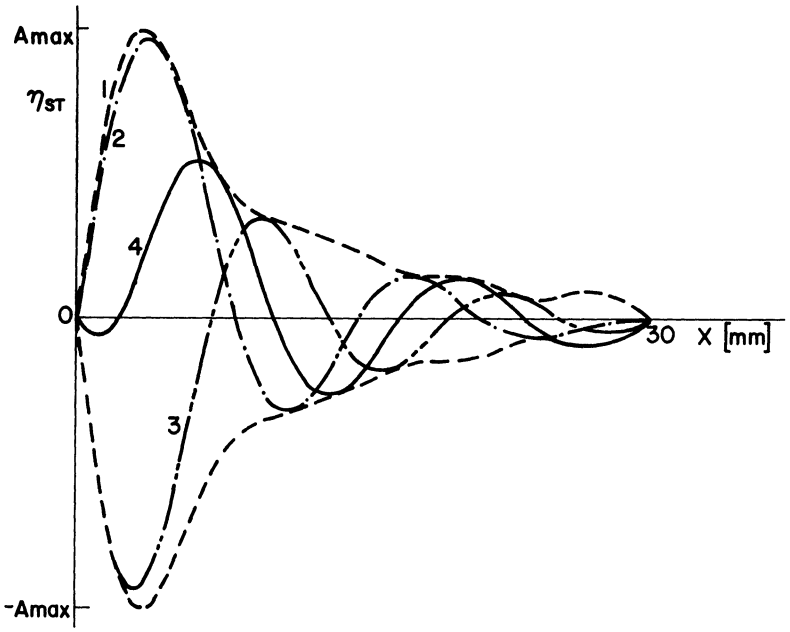

FIG. 2. *Curves contributing to the steady state displacement envelope* (*curve* 1). *Curves correspond to time values in seconds*: *curve* 2 = 1.567×10^{-6}, *curve* 3 = 1.567×10^{-4}, *curve* 4 = 1.567×10^{-2}, *and* $\omega = 2.5$ khz

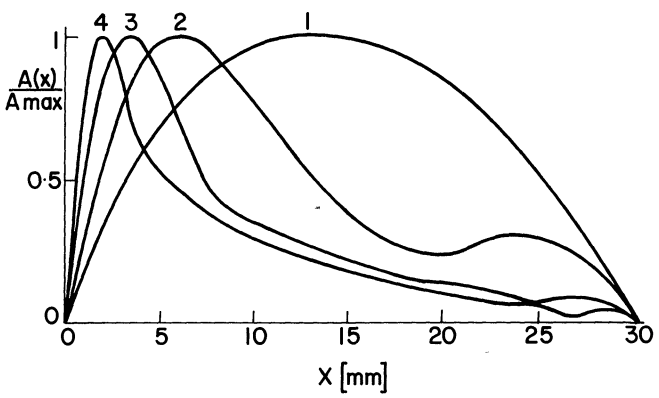

FIG. 3. *Steady state normalized displacement envelopes. Curves correspond to different frequencies in* hz: *curve* 1 = 25, *curve* 2 = 250, *curve* 3 = 2,500, *curve* 4 = 25,000

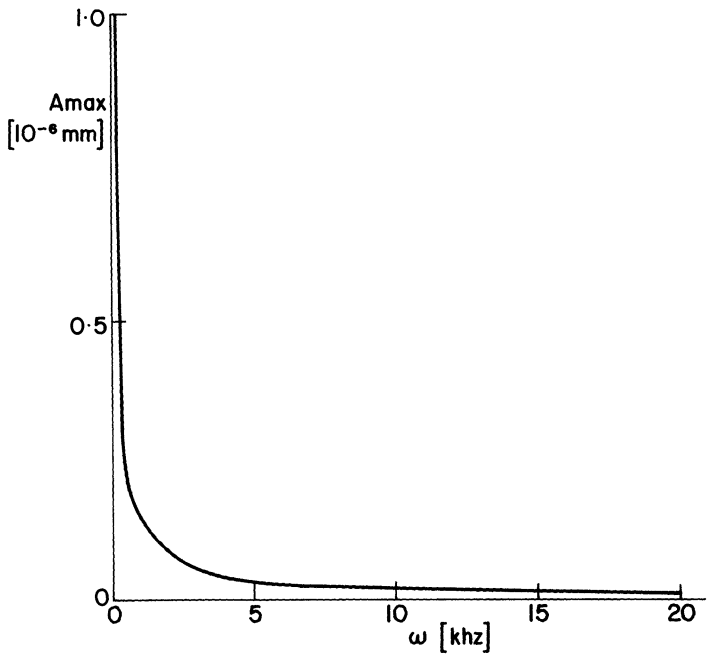

FIG. 4. *Magnitude of maximum of displacement envelope as a function of driving frequency.* $d = 0.08 \times 10^{-3}$ m

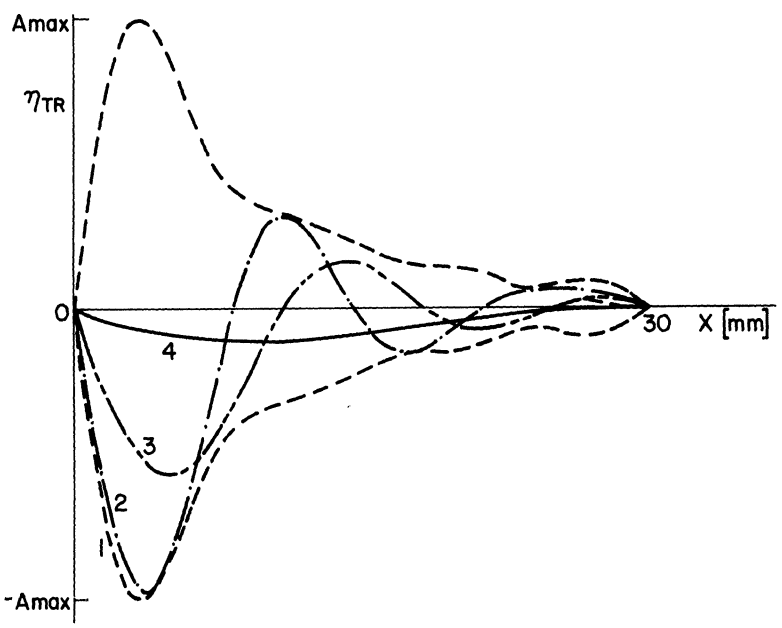

FIG. 5. *Transient curves within steady state displacement envelope (curve* 1*). Curves correspond to time values in seconds: curve* 2 = 1.567×10^{-6}, *curve* 3 = 1.567×10^{-4}, *curve* 4 = 1.567×10^{-2} *and* $\omega = 2.5$ khz

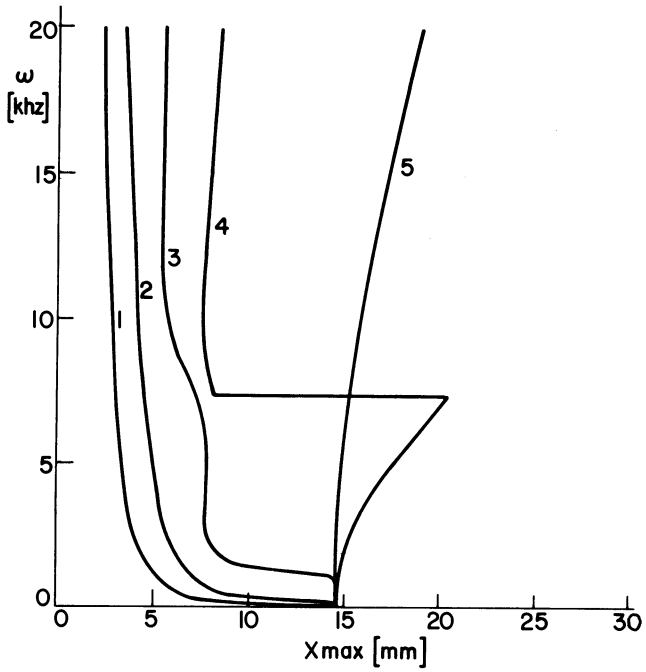

FIG. 6. *Positions along membrane of displacement envelope maxima as a function of driving frequency (Place principle). Curves correspond to different values of the elastic modulus E in* N/m^2: *curve* 1 = 1.4×10^{13}, *curve* 2 = 1.4×10^{14}, *curve* 3 = 1.4×10^{15}, *curve* 4 = 1.4×10^{16}, *curve* 5 = 1.4×10^{17} *and* $d = 0.08 \times 10^{-3}$ m

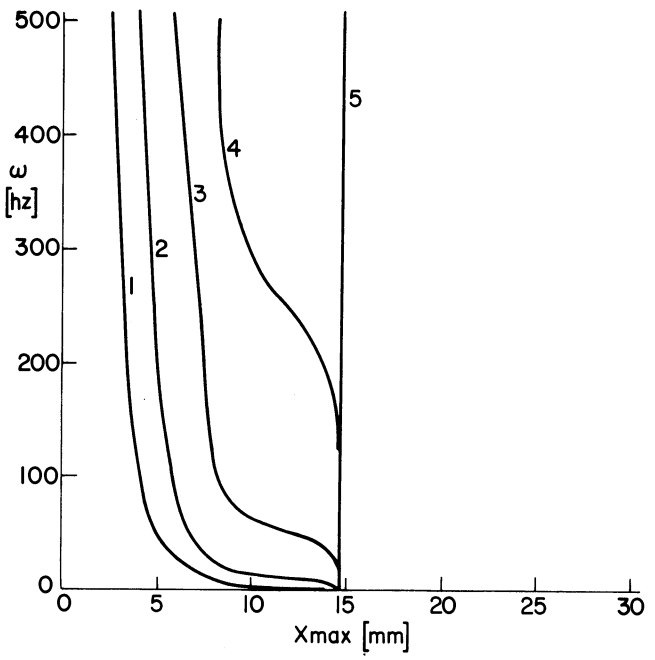

FIG. 7. *Positions along membrane of displacement envelope maxima as a function of driving frequency (Place principle at low frequency). Curves correspond to different values of the elastic modulus E in* N/m^2: *curve* 1 = 1.4×10^{11}, *curve* 2 = 1.4×10^{12}, *curve* 3 = 1.4×10^{13}, *curve* 4 = 1.4×10^{14}, *curve* 5 = 1.4×10^{15} *and* $d = 0.08 \times 10^{-3}$ m

TABLE 1
Values of parameters used in computation

Parameter	Value
Chamber height, h	0.2×10^{-3} m
Beam thickness, d	0.06×10^{-3} m
Modulus of elasticity, E	1.4×10^{13} N/m^2
Density of fluid, ρ	1×10^3 kgm/m^3
Density of beam, ρ_b	1×10^3 kgm/m^3
Length of beam, L	30×10^{-3} m
Kinematic viscosity, ν	3×10^{-3} m^2/sec

given in Table 1, unless explicitly stated otherwise. The modulus of elasticity of the beam was typically very large, 1×10^{13}N/m^2. This suggests that an elastic plate supported along its lengthwise edges would be a more appropriate model of the basilar membrane. Such a plate has the required stiffness but with a smaller value of the modulus of elasticity. Also the viscosity (required to get a Place principle) of the fluid (~ 30 poise) was much greater than that reported by von Bekesy [4] for the perilymph. However, this high viscosity agrees with his description of the contents of the scala media as a "gelatinous mass", which indicates that substantial damping takes place in the scala media which is not accounted for in this model.

Steady state waves traveling inside their envelope are shown in Fig. 2. In all cases, the wave travel increases with frequency. In an inviscid fluid, the steady state beam oscillations are standing waves. This can be easily seen from (7) and (8) where d_{2n} vanishes when $\nu = 0$. Viscous damping increases with frequency by (22) in [1]. Hence the wave travel increases with frequency. With a nontapered geometry, viscous damping is a crucially needed element for a Place principle to exist since without it, strong multiple peaks easily form in the envelope. This result is interesting in that it is in direct contrast to the previously accepted role of viscosity. For example, Wever [8] argues that viscous damping seriously limits mechanical localization in the cochlea to such an extent that it becomes necessary to favor a "frequency theory" of hearing over a "place theory".

The upper half of the normalized envelopes of steady state waves with single strong maxima are shown in Fig. 3 for various frequencies. The place of the strong maximum moves distinctly to the left with increasing frequency. The peaks also get notably sharper with increasing frequency. As explained in § 1.5, the maxima of the low frequency envelopes are located near the center of the beam. The functional significance of the increasing width of the human basilar membrane in the apical direction is primarily to shift the low frequency maxima farther to the right, which increases the tonal differentiation. It is possible to shift the low frequency response into the right half of the beam with this model, but invariably there is an erratic movement of the maxima for these cases (see curve 4 of Fig. 6). As shown in § 1.4, even in these cases, $x_{\max} \to 0$ as $\omega \to \infty$.

Figure 4 shows that the magnitude of the envelope maxima is a strong monotone decreasing function of frequency. This behavior is in part due to the assumed hinged end conditions of the beam, together with the assumption that the beam is

not tapered. The low frequency maxima occur near the center of the beam where the displacements are large compared to the displacements near the left hinge, which is the location of activity of the high frequency sounds. Therefore, the high frequency auditory threshold, besides being a result of severely diminished sensitivity, is also caused by an insufficient displacement of the basilar membrane.

This behavior, as exhibited in Fig. 4, raises some interesting questions concerning the characteristics of the hair cell receptors of the organ of Corti. This curve suggests that these receptors do not respond to the absolute magnitude of the envelope, since the amplitude of a point on the beam distant from the maxima for a low frequency signal can be orders of magnitude larger than the maximum amplitude for a higher frequency. This strongly suggests that these receptors are coupled in a network which can detect relative maxima, as previously suggested by Huggins and Licklider [9]. Another attractive idea for the stimulation of the receptors has been recently given by Steele [10], who suggests that a maximum in the displacement of the basilar membrane locally creates a venturi effect which produces a subtectorial membrane fluid stream in a direction *across* the width of the basilar membrane.

The response of the transient part of the solution for an input frequency of 2500 hz is shown in Fig. 5. The wave is effectively damped out after 15 milliseconds. The rate of decay increases with the frequency of the input signal, indicating that the ear is well suited to respond to rapidly changing sounds. The transient part of the solution does not effect the envelope nor the Place principle as explained in § 1.3.

The existence of a Place principle is clearly illustrated in Figs. 6 and 7, where the position of the envelope maximum $x_{\max}$ varies with the frequency of the input signal. Vertical regions of the curves where $d\omega/dx_{\max} \to \infty$ indicate very poor sensitivity, i.e., the position of the envelope maximum does not change significantly with frequency. These regions occur at low and high frequencies and thus define audio thresholds in terms of severely limited sensitivity. As explained in § 1.4 and 1.6, $d\omega/dx_{\max} \to \infty$ as $\omega \to 0$ and $\omega \to \infty$. For some parameter values, vertical slopes occur for intermediate frequencies (see Fig. 6, curve 3). Such regions define impaired hearing with a bandwidth given by the extent of the vertical region. (It is indeed intriguing to operate the interactive graphic display of these curves and to remove these areas of reduced sensitivity by changing parameter settings.)[2] Regions of horizontal slopes indicate high sensitivity. However, the horizontal portion of curve 4 in Fig. 6 is not a region of high sensitivity. Rather, it is an artifact caused by the presence of two equal relative maxima at $\omega \sim 7$ khz. Above and

[2] The computations were performed on an IBM system 370/145 computer via an IBM 2741 Communications Terminal. All programs were written exclusively in APL using the APL (CMS) Installed User Program under an IBM Virtual Machine Facility/370 time sharing system. Thus it became possible by use of a TSP-12 Plotter Controller and Tektronix-611 Storage Tube Display to interactively develop parameter values through interpretation of wave forms. Since each computation involved the sum of a possibly oscillating series, the sum of an analogous series of positive terms was calculated simultaneously, stopping when the nth term became less than one-tenth of one percent of the accumulated sum. The array handling capabilities of APL permitted the programs to perform the series calculation in parallel for a vector of x values, making it more efficient to calculate the maximum of a curve simply by evaluation rather than by an iterative algorithm. The programs also generated and stored the data in CMS disk files for subsequent retrieval.

below that frequency, there exist unique absolute maxima. The Place principle at low frequency is shown in Fig. 7. It is apparent in some of the curves that $d\omega/dx_{max} \to \infty$ as $\omega \to 0$, which illustrates the low frequency sensitivity threshold.

No attempt has been made to compare these results with existing physiological data. The model is still too crude for quantitative comparisons. Nevertheless, this model clarifies the general aspects of the mechanics of the cochlea. The model will hopefully stand up to comparison with physiological data when the effects of tapered geometry are included. Since these nonuniformities are slowly varying functions of position, it is not anticipated that such a refinement will lead to a fundamentally different qualitative behavior of the cochlea.

3. Summary. The following points concerning the mechanics of the cochlea are demonstrated by this mathematical model.

(a) Traveling waves exist in the basilar membrane, and are a direct result of the viscosity of the fluid.

(b) A Place principle, defined in terms of the location of the maximum of the wave envelope of the basilar membrane, exists in the uniform cochlea, and only if viscosity is present.

(c) Transient waves have no effect on either the wave envelope or the Place principle.

(d) There exist low and high frequency thresholds defined in terms of severely limited sensitivity to tonal differentiation. The high frequency threshold is also a result of small basilar membrane displacements.

(e) The real basilar membrane is tapered (see Fig. 8) such that low frequency

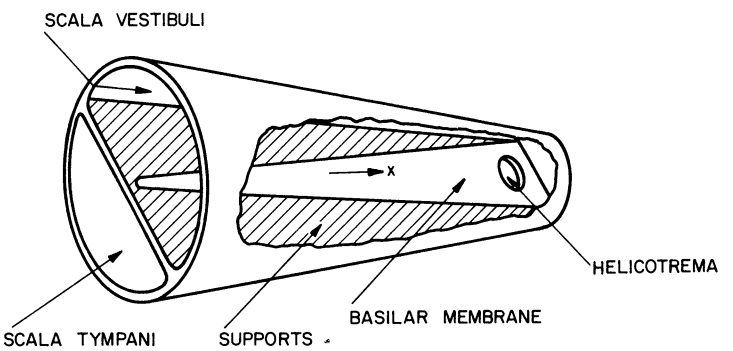

FIG. 8. *Schematic of uncoiled cochlea (scala media not shown for clarity). The width of the basilar membrane increases with x, while the cross-sectional area of the cochlear ducts decrease with x*

envelope maxima can occur near the helicotrema. Thus the tapered membrane is active (i.e., envelope maxima occur) over the entire length. The uniform membrane is active only on the stapes half, which results in a poorer sensitivity to tonal differentiation than the tapered membrane.

(f) The cochlear ducts (see Fig. 8) are also tapered with a smaller cross-sectional area near the helicotrema than the stapes. One reason for this taper is,

of course, to pack the actual coiled structure of the cochlea into the surrounding bone in an efficient manner. It is interesting to speculate, however, that the taper of the cochlear duct compensates for the taper of the basilar membrane in such a way that the high frequency response is unaffected by (e), i.e., the increased normal velocity gradient of the fluid near the helicotrema increases the damping at this location at high frequency. (Also, the tapered ducts improve the pressure loading at low frequency by increasing the net pressure difference near the helicotrema.) Thus, it is conjectured that the tapered cochlear ducts tend to preserve the high frequency response of the oppositely tapered basilar membrane, and improve the low frequency response.

Acknowledgments. We are indebted to the following individuals and organizations for their cooperation and invaluable assistance in the course of this work.

The IBM Corp. (U.S.A.) through its Los Angeles Scientific Center (LASC) has graciously supported this research. Messrs. W. Wangel, J. Hinchcliffe and G. Rathe of IBM and Drs. H. H. Givin, L. Leeburg and A. Hurwitz of IBM-LASC have enthusiastically and consistently given us of their time, efforts, and skills.

The Ear Research Institute through Drs. J. Pulec, F. Linthicum and W. House, provided their vast clinical experience and insight.

Professor J. Tondorff of Columbia University Medical School and Professor K. Stewartson of University College, London, participated in critical discussions and made many valuable suggestions.

The Technion Research Foundation partially supported this effort.

We gratefully acknowledge the referee's comments and suggestions which have substantially improved these papers.

Any errors and shortcomings are, of course, the responsibility of the authors.

REFERENCES

[1] A. INSELBERG AND R. S. CHADWICK, *Mathematical model of the cochlea. I: Formulation and solution*, this Journal, 30 (1976), pp. 149–163.

[2] A. F. HUXLEY, *Is resonance possible in the cochlea after all?*, Nature, 221 (1969), pp. 935–940.

[3] E. G. WEVER AND M. LAWRENCE, *Physiological Acoustics*, Princeton University Press, Princeton, N.J., 1954.

[4] V. VON BEKESY, *Experiments in Hearing*, McGraw-Hill, New York, 1960

[5] L. B. W. JOLLEY, *Summation of Series*, No. 533, Dover, New York, 1961.

[6] A. INSELBERG AND H. VON FOERSTER, *A mathematical model of the basilar membrane*, Math. Biosci. 7 (1970), pp. 341–363.

[7] "HUTTE", *Des Ingenieurs Taschenbuch*, No. 12, W. Ernst, Berlin, 1948.

[8] E. G. WEVER, *Theory of Hearing*, Dover, New York, 1949.

[9] W. H. HUGGINS AND J. C. R. LICKLIDER, *Place mechanisms of auditory frequency analysis*, J. Acoust. Soc. Amer., 23 (1951), pp. 290–299.

[10] C. R. STEELE, *A possibility for sub-tectorial membrane fluid motion*, Basic Mechanisms in Hearing, A. R. Møller, ed., Academic Press, New York, 1973, pp. 69–93.